Received: 2 December 2020 | Revised: 8 April 2021 | Accepted: 9 April 2021

DOI: 10.1002/psp4.12639

ARTICLE

Population pharmacokinetic modeling of molibresib and its active metabolites in patients with solid tumors: A semimechanistic autoinduction model

Anu Shilpa Krishnatry[1] | **Alexander Voelkner**[2] | **Arindam Dhar**[3] | **Marita Prohn**[2] | **Geraldine Ferron-Brady**[1]

[1]Clinical Pharmacology Modelling and Simulation, GlaxoSmithKline, Collegeville, PA, USA

[2]qPharmetra LLC, Nijmegen, the Netherlands

[3]Epigenetics Research Unit, GlaxoSmithKline, Collegeville, PA, USA

Correspondence
Anu Shilpa Krishnatry, Clinical Pharmacology Modelling and Simulation, GlaxoSmithKline, 1250 S Collegeville Rd, Collegeville, PA 19426, USA.
Email: anu.s.krishnatry@gsk.com

Funding information
This study was funded by GlaxoSmithKline (115521; NCT01587703).

Abstract

Molibresib (GSK525762) is an investigational, orally bioavailable, small-molecule bromodomain and extraterminal (BET) protein inhibitor for the treatment of advanced solid tumors. Molibresib was initially evaluated in a first-time-in-human (FTIH) study BET115521 consisting of two parts: Part 1 of the study (dose escalation) was conducted in 94 patients with nuclear protein in testis midline carcinoma and other solid tumors, and Part 2 (expansion cohort) was conducted in 99 patients with different solid tumor types. Molibresib is metabolized by cytochrome P450 3A4 enzymes to produce two major active metabolites that are equipotent to the parent molecule. The metabolites are measured together after full conversion of one to the other and reported as an active metabolite composite (GSK3529246). The molibresib pharmacokinetic (PK) profile has been characterized by a decrease in exposure over time, with the decrease more pronounced at higher doses, and accompanied by a slight increase of the metabolite concentrations. Autoinduction of molibresib metabolism was suspected and confirmed *in vitro*. Here we report the development of a semimechanistic liver-compartment population PK model using PK data from the FTIH study, which adequately describes the autoinduction of molibresib clearance and the PK of both molibresib and GSK3529246. Covariate analysis indicated body weight had a significant effect on the volume of distribution of molibresib and GSK3529246, and higher levels of aspartate aminotransferase resulted in the lower clearance of GSK3529246. This model was used to simulate individual patient exposures based on covariate information for use in future alternative dosing strategies and exposure–response analyses.

Study Highlights

WHAT IS THE CURRENT KNOWLEDGE ON THE TOPIC?

Molibresib, being developed for the treatment of solid tumors, has two major active metabolites that are equipotent to molibresib. Previous *in vitro* studies and

This is an open access article under the terms of the Creative Commons Attribution-NoDerivs License, which permits use and distribution in any medium, provided the original work is properly cited and no modifications or adaptations are made.
© 2021 The Authors. *CPT: Pharmacometrics & Systems Pharmacology* published by Wiley Periodicals, Inc. on behalf of the American Society for Clinical Pharmacology and Therapeutics.

pharmacokinetic (PK) analyses indicated the potential for autoinduction of molibresib metabolism.

WHAT QUESTION DID THIS STUDY ADDRESS?

This analysis investigated the development of a semimechanistic liver-compartment model to describe the population PK of molibresib and its active metabolite composite GSK3529246.

WHAT DOES THIS STUDY ADD TO OUR KNOWLEDGE?

We developed a semimechanistic population PK model with a liver-compartment to describe autoinduction of molibresib clearance and the PK of both molibresib and GSK3529246. In addition, body weight was identified as a covariate that affected the volume of distribution for molibresib and GSK3529246; time-varying aspartate aminotransferase was identified as a covariate on metabolite clearance.

HOW MIGHT THIS CHANGE DRUG DISCOVERY, DEVELOPMENT, AND/OR THERAPEUTICS?

This model is a useful tool to predict patient exposure of molibresib and GSK3529246 based on covariate information to aid future dosing and combination strategies. The model can also be applied to other compounds exhibiting autoinduction.

INTRODUCTION

Molibresib (GSK525762) is an investigational, orally bioavailable, small-molecule bromodomain (BRD) and extraterminal (BET) protein inhibitor[1,2] for the treatment of advanced solid tumors and hematologic malignancies. BRDs are small conserved functional motifs found in a variety of human proteins,[3] which act as epigenetic readers that regulate the expression and transcription of a number of genes controlling growth and cell cycle progression and differentiation,[4–8] and members of the BET family of BRDs have been implicated in tumorigenesis.[3,9] Preclinical studies have shown that molibresib inhibits the proliferation of human cell lines derived from nuclear protein in testis carcinoma (NC),[10] small cell lung cancer (SCLC),[11] castration-resistant prostate cancer (CRPC),[12,13] triple negative breast cancer (TNBC),[14,15] estrogen receptor positive breast cancer (ER+BC),[15,16] and gastrointestinal stromal tumor (GIST).[17]

To expand on these initial preclinical findings, a two-part, first-time-in-human (FTIH) phase I/II study investigated the safety, pharmacokinetic (PK) profile, pharmacodynamics, and clinical activity of molibresib in patients with NC and other solid tumors (NCT01587703; BET115521).[18] The aim of Part 1 ($n = 94$) was to determine the recommended phase II dose (RP2D) of molibresib. Patients in the Part 1 dose-escalation portion of the study received molibresib doses of 2–100 mg once daily (q.d.; $n = 65$) as an amorphous free-base formulation.[18] In addition, twice-daily dosing ($n = 19$) was evaluated (unpublished data on file), and a cross-over bioavailability study of the Part 1 amorphous free-base and the Part 2 besylate salt formulations ($n = 10$) was carried out in Part 1 (G. Ferron-Brady et al., unpublished data). Based on the findings from Part 1, a 75 mg q.d. dose of the besylate formulation of molibresib[18] was selected for Part 2 of the study ($n = 99$) to further investigate the use of molibresib in patients with NC, SCLC, CRPC, TNBC, ER+BC, and GIST (S. Cousins et al., unpublished data).

The molibresib PK profile is characterized by rapid absorption and elimination, with the maximum plasma concentration (C_{max}) occurring within 2 h post dose and a terminal half-life ($t_{1/2}$) of 3–7 h.[18] Molibresib is an *in vitro* substrate of human cytochrome P450 3A4 (CYP3A4), as demonstrated in a study using human liver microsomes that showed predominantly CYP3A4-mediated metabolism of molibresib.[19] In addition, physiologically based PK (PBPK) modeling of molibresib using data from a two-part, randomized, open-label, crossover drug–drug interaction trial confirmed the major role of CYP3A enzymes in molibresib metabolism and clearance.[19] Molibresib has also been shown to be a substrate of the P-glycoprotein transporter *in vitro*.[19]

Molibresib is metabolized by CYP3A4 into two active major metabolites (GSK3536835 [ethyl hydroxy] and GSK3529246 [N-desethyl]),[19] which have both shown similar inhibitory potency against tumor cell lines to the parent molecule[18] and were measured together following full conversion of GSK3536835 to GSK3529246 and reported as an active metabolite composite, GSK3529246.[18,19] The free fraction in plasma for both molibresib and GSK3529246 has been shown to be approximately 0.2.[19] In Part 1 of the FTIH study, molibresib PK was characterized by a decrease in molibresib exposure (which was more pronounced at doses ≥60 mg q.d.) and accompanied by a slight increase in GSK3529246 concentration over time.[18] The apparent autoinduction of molibresib metabolism was shown to be mediated by CYP3A4, whose expression in primary human hepatocytes has been shown to increase *in vitro* with higher levels of molibresib (unpublished data on file). An empirical model was developed to describe the autoinduction of molibresib clearance using preliminary data from Part 1 of the

FTIH study.[20] This model included induced/preinduced clearance, an induction lag time, and a turnover rate for the induced enzyme.[20] However, the data did not support a more mechanistic model.[20] In the analysis reported herein, we aimed to (i) develop a population PK model of molibresib and GSK3529246 in patients with solid tumors using data from Part 1 and Part 2 of the BET115521 study, (ii) describe the observed autoinduction semimechanistically, and (iii) identify covariates of clinical interest. The model was subsequently used to generate exposure values for use in subsequent exposure–response analyses for safety end points, the results of which will be reported separately (A.S. Krishnatry et al., unpublished data).

METHODS

Patients and study design

Population PK analysis was performed on plasma samples obtained from the multicenter, open-label, two-part phase I/II FTIH study BET115521 investigating the use of molibresib in patients with NC and other solid tumors. Details on the design and methodology for the FTIH study have been published previously.[18] Briefly, Part 1 of the study was a dose-escalation phase involving single-dose and repeat-dose oral administration of 2–100 mg molibresib as an amorphous free-base formulation to evaluate the safety, PK, and pharmacodynamics of molibresib and to determine the RP2D.[18] Part 2 of the study assessed the efficacy, safety, PK, and pharmacodynamics of molibresib as a besylate salt formulation at the RP2D of 75 mg once daily in patients with NC and other solid tumors (S. Cousins et al., unpublished data). The study was conducted in accordance with International Conference on Harmonisation Good Clinical Practice and applicable country-specific regulatory requirements as well as the ethical principles outlined in the Declaration of Helsinki 2008. All participants provided written informed consent before study enrollment.

PK sampling and bioanalysis

PK analysis was performed on plasma from all patients in the BET115521 study who received at least one dose of molibresib and provided viable blood samples. Extensive PK samples were obtained after a single dose (Week 1, Day 1) and repeated dosing (Week 3, Day 4) with other samples taken less frequently at other time points throughout treatment (Table S1). Molibresib concentration was analyzed in all patients ($n = 193$), whereas GSK3529246 concentration was analyzed in all Part 2 ($n = 99$) and Part 1 80 mg ($n = 32$) patients only (Table S2). Molibresib and GSK3529246 plasma concentrations were analyzed using a validated method based on liquid–liquid or protein precipitation extraction, followed by ultra-high performance liquid chromatography with tandem mass spectrometry.[18] Molibresib and GSK3529246 postdose PK observations that were below the lower limit of quantification (LLOQ; molibresib LLOQ: 0.2–1.0 /ml; GSK3529246 LLOQ: 1 ng/ml) were excluded from the analysis. No imputations were performed for missing data; observations with missing PK or time values were excluded. PK observations were omitted from the analysis if dose information was missing or if the dosing time was unclear. Any patients who required dose interruptions or dose reductions were included in the population PK analysis at the dose they received, taking into account individual dosing fluctuations and interruptions. In addition, observation records with quantifiable predose concentrations and date and time errors in the data sets were excluded.

PK modeling criteria for model building and software

The population PK analysis was performed using a nonlinear mixed-effect modeling approach using NONMEM version 7.4 (Icon Development Solutions, Ellicott City, MD). Model development was performed using first-order conditional estimation with η–ε interaction. Model execution and visual predictive checks (VPC) were performed using Perl-speaks-NONMEM version 4.8.0,[21] and postprocessing of NONMEM analysis data was completed using R version 3.5.2.[22] The following modeling assumptions were made for a typical patient: (i) a hepatic blood flow of 100 L/h and an average hematocrit of 45%,[23,24] resulting in a hepatic plasma flow of 55 L/h; (ii) a liver volume of 1.5 L[25]; and (iii) a fraction metabolized of 1. Further assumptions and justifications are detailed in Table S3. The selection of models was based on a difference in objective function value (OFV) of 6.63 (equivalent to a $p < 0.01$) to compare any two nested models that differed by one parameter. The same process was applied to models that differed by two parameters using an OFV threshold of 9.21 (also equivalent to $p < 0.01$).[26] The accepted model was then determined on the basis of the lowest stable OFV, physiological plausibility of parameter values, successful numerical convergence, parameter precision, and acceptable prediction-corrected VPC outcomes.[27]

Structural PK model

Models were developed in increasing order of complexity, starting with simple models (e.g., a one-compartment model with first-order absorption kinetics using only molibresib PK observations) and proceeding until further improvement in the model fit was not supported by the data. This approach was applied to (i) the search for structural model components (e.g., the number of apparent distribution components) and the assessment of random effects (residual

variability and interindividual variability [IIV]) to create the structural model and (ii) the evaluation of clinical covariate effects on molibresib metabolism. Following identification of a structural model for the PK of molibresib, GSK3529246 PK observations were included to form a combined structural PK model, simultaneously describing the plasma concentrations over time for both molibresib and GSK3529246. Plasma concentrations were converted in molar concentrations using the molecular weights of molibresib (424 g/mol) and GSK3529246 (396 g/mol) for the modeling. Model refinement was based on the change in OFV and/or the model qualification assessments described in "Covariate analysis and final PK model development".

Covariate analysis and final PK model development

Once the combined structural PK model had been identified, a generalized additive model (GAM) approach was used to identify clinical covariates that were most likely to affect the apparent molibresib clearance (CL/F), apparent molibresib central volume of distribution (V_1/F), apparent GSK3529246 clearance (mCL/F), and apparent GSK3529246 central volume of distribution (mV_1/F). Covariates evaluated in the GAM analysis were dose, age, weight, sex, race, ethnicity, baseline body mass index, baseline body surface area, alanine aminotransferase (ALT), baseline ALT, aspartate aminotransferase (AST), baseline AST, baseline albumin, baseline bilirubin, cancer type, baseline Eastern Cooperative Oncology Group status, liver metastasis, history of liver reduction surgery, FTIH study part, comedication, smoking status, prior taxane-based chemotherapy, and prior platinum-based chemotherapy. Covariates were only carried forward if they had a corresponding p value < 0.01 (OFV change of >6.63 with one degree of freedom). All identified covariates from the GAM analysis were then incorporated into the full covariate PK model, and a stepwise backward elimination was performed until removal of a particular covariate resulted in a statistically significant ($p < 0.001$; OFV change of 10.8 with one degree of freedom) change in the model fit. Continuous covariates, X_i, on a particular model parameter, P_i, were included in the full model using a power model:

$$P_i = P_{TV}\left(\frac{X_i}{\%X}\right)^{\theta_X}$$

in which θ_X is the power estimate for the covariate effect and $\tilde{X}$ is the median value of the covariate. The impact of statistically significant covariates on the PK parameters were illustrated as the difference to the median values of the covariate. For the continuous covariates, the 5th and 95th percentiles were compared with the median and illustrated including uncertainty (90% confidence interval) to estimate the covariate effect. A total of 1000 sets of parameter estimates (using the estimated uncertainty from the $COV step in NONMEM) were used.

Model qualification

Following covariate analysis, the final population PK model was qualified using graphical and numerical goodness-of-fit (GOF) analyses and prediction-corrected VPC. Graphical GOF analysis involved inspecting diagnostic plots of observed versus predicted values to determine any evidence of systemic lack of fit or bias in the error distributions. Numerical GOF was determined based on successful numerical convergence, acceptable parameter precision (a relative standard error <50%), a low condition number (<1000), and biological plausibility of the PK parameter values. Prediction-corrected VPCs,[21] stratified by covariates of interest, were created.

Exposure predictions

Individual *post hoc* PK parameter estimates were obtained using the final PK model and used to simulate hourly molibresib, active metabolite composite (GSK3529246), and total active moiety (TAM) concentrations for the entire course of treatment (FTIH study). The simulations accounted for individual dosing histories and covariates of interest, and exposure metrics (C_{max}, minimum plasma concentration [C_{min}], and area under the concentration–time curve [AUC]) were derived for both single (Week 1, Day 1) and repeat (Week 3, Day 4) dosing stratified by study cohort and dose. The AUC was calculated using the trapezoidal method from hourly predicted concentrations.

RESULTS

Analysis population

Demographics, prior treatments, and clinical characteristics at baseline for patients included in the PK population are summarized in Table 1. The study population had a median age (range) of 58 years (16–86) and were predominantly White (83%) with a median (range) body weight of 69.6 kg (34–120 kg). In total, 2681 molibresib and 814 active metabolite PK observations from 193 patients were included in the analysis for model development. Of these, 260 molibresib and 144 GSK3529246 PK observations were below the LLOQ, and 25 observation records with quantifiable predose concentrations and date and time errors were excluded. The majority of

TABLE 1 Demographics and clinical characteristics at baseline for the PK population (FTIH study)

Demographic/characteristic[a]	Part 1 q.d. (*N* = 65)	Part 1 b.i.d. (*N* = 19)	Besylate substudy (*N* = 10)	Part 2 (*N* = 99)	Total study (*N* = 193)
Age, years	50.8 (17)	63.3 (7.2)	55.2 (10)	57.6 (12)	55.7 (14)
Sex, female, n (%)	31 (48)	7 (37)	5 (50)	60 (61)	103 (53)
Race, n (%)					
Asian	3 (5)	1 (5)	0	8 (8)	12 (6)
Black or African American	5 (8)	0	1 (10)	6 (6)	12 (6)
White	56 (86)	18 (95)	9 (90)	77 (78)	160 (83)
Missing	1 (2)	0	0	8 (8)	9 (5)
Weight, kg	73.5 (18)	69.5 (15)	76.8 (8.1)	70.4 (17)	71.7 (17)
Body mass index, kg/m^2	25.3 (4.8)	24.3 (3.9)	26.2 (2.9)	25.2 (5.3)	25.2 (4.9)
Body surface area, m^2	1.86 (0.27)	1.8 (0.24)	1.92 (0.13)	1.81 (0.26)	1.83 (0.26)
Total bilirubin, mg/dL	0.51 (0.3)	0.48 (0.26)	0.59 (0.26)	0.483 (0.2)	0.498 (0.25)
ALT, IU/L	32.9 (44)	25.5 (13)	24.9 (16)	24.6 (15)	27.5 (28)
AST, IU/L	35.2 (22)	34.9 (13)	32.7 (17)	32.6 (18)	33.7 (19)
ECOG performance status, n (%)					
0	22 (34)	10 (53)	3 (30)	29 (29)	64 (33)
1	40 (62)	9 (47)	7 (70)	69 (70)	125 (65)
2	3 (5)	0 (0)	0 (0)	1 (1)	4 (2)
Tumor type, n (%)					
Breast	5 (8)	1 (5)	0	38 (38)	44 (23)
Colon/rectum	22 (34)	14 (74)	9 (90)	0	45 (23)
GIST	0	0	0	13 (13)	13 (7)
Lung	8 (12)	1 (5)	0	14 (14)	23 (12)
Multiple myeloma	1 (2)	0	0	0	1 (<1)
Neuroblastoma	1 (2)	1 (5)	0	0	2 (1)
NC	19 (29)	0	0	11 (11)	30 (16)
Prostate	9 (14)	2 (11)	1 (10)	23 (23)	35 (18)
Prior cancer-related therapy, n (%)					
Platinum based	51 (79)	18 (95)	9 (90)	52 (53)	130 (67)
Taxane based	23 (35)	4 (21)	1 (10)	70 (71)	98 (51)

Abbreviations: ALT, alanine aminotransferase; AST, aspartate aminotransferase; b.i.d., twice daily; ECOG, Eastern Cooperative Oncology Group; FTIH, first time in humans; GIST, gastrointestinal stromal tumor; NC, nuclear protein in testis carcinoma; PK, pharmacokinetic; q.d., once daily.

[a]Data are presented as mean (standard deviation) unless otherwise stated.

patients received 80 mg q.d. of the amorphous free-base formulation or 75 mg q.d. of the besylate salt formulation (Table S2). Exploratory analysis of extensive PK data obtained in Part 1 of the study (80 mg q.d.) indicated multiphasic drug disposition with a decrease in molibresib exposure, a slight accumulation of GSK3529246, and a decrease in TAM at steady-state exposures, suggesting autoinduction (Figure S1).

Structural PK model development

The key steps for building a combined structural PK model for molibresib and GSK3529246 (including the initial molibresib-only model) are shown in Table 2, and comprehensive details of the step-by-step development process are presented in Supplementary Text S1. Starting with a one-compartment model, random effects were then included on the absorption rate constant (ka), CL/F, and V_1/F. Adding a peripheral compartment and absorption lag time significantly improved the model fit. Further model development included changes based on molibresib clearance over time, dose, or concentration. Overall, a physiologic liver model, in which enzyme induction was driven by the amount of molibresib in the liver, resulted in the best fit of the data and was taken forward to further develop the combined PK model.

TABLE 2 Summary of modeling steps for the (a) molibresib-only and (b) combined structural PK models

Molibresib-only structural model					
Run	**Ref**	**ΔOFV**	**Minimization**	**Description**	**Action**
100			Successful	One-compartment model (no IIV)	
101	100	−4157.3	Successful	One-compartment model (IIV CL/F, V_1/F, ka)	Accepted
102	101	−488.2	Successful	Two-compartment model (IIV CL/F, V_1/F, ka)	Accepted
103	102	−128.1	Successful	Run 102 + lag time	Accepted
104	103	0	Rounding error	Rerun of 103 with ADVAN13	Accepted
105	104	−327.1	Successful	Run 104 + induction compartment with linear induction	Accepted
106	105	−1.1	Successful	Run 104 + induction compartment with IMAX effect	Rejected
107	106	−66.5	Successful	Liver model	**Selected**
108	107	–	Successful	Rerun of Run 107 with full data set	Rejected
Molibresib and GSK3529246 combined structural model					
Run	**Ref**	**ΔOFV**	**Minimization**	**Description**	**Action**
1			Failed	Run 107 and two-compartment model for GSK3529246	
2	1	−148.8	Successful	Run 1, add correlation for residual error	Accepted
4	2	−165.8	Successful	Run 2, replace absorption with GSK3529246 formation from liver	Accepted
5	4	17.4	Rounding error	Run 4, fix induction k_{in} to 0.0055	Accepted
6	5	−2.1	Successful	Run 5, but induction effect on mCL/F (same slope)	Rejected
7	5		Successful	Run 5, using full data set and estimate k_{in}	Rejected
8	5	441.2	Failed	Run 5, with induction on mCL/F only	Rejected
9	5	41.7	Successful	Run 5, no IIV on mka	Rejected
10	5	249.6	Successful	Run 5, remove GSK3529246 peripheral compartment	Rejected
12	5	−10.2	Successful	Rerun Run 5 with smaller lower boundary for induction slope	Accepted
14	12	−46.4	Successful	Run 12, add weight on V_1/F and mV_1/F	**Selected**

Note: For the molibresib-only structural model, Run 107 was selected. For the combined structural model, Run 1 consisted of the structural molibresib-only model plus a separate two-compartment model for GSK352924 with IIV on mCL/F, mV_1/F, and ka.

Abbreviations: ΔOFV, change in objective function compared with reference model; ADVAN13, implementation with differential equations in NONMEM; CL/F, apparent molibresib clearance; E_{max}, maximal effect; IIV, interindividual variability; IMAX, inhibitory E_{max}-model model; ka, absorption rate constant; k_{in}, enzyme production rate; mCL/F, GSK3529246 clearance; mka, GSK3529246 absorption rate; mV_1/F, GSK3529246 central volume; OFV, objective function value; PK, pharmacokinetic; Ref, reference model; V_1/F: molibresib central volume; WT, weight.

For the combined structural model, starting with separate molibresib and GSK35292426 two-compartment submodels, random effects (IIV) were included for mCL/F, mV_1/F, and the GSK3529246 ka, and residual variability was described by proportional error models. Subsequent steps that improved the model fit were the following: (i) the inclusion of residual error correlation for molibresib and GSK3529246 (Run 2); (ii) replacing the absorption with the molibresib to GSK3529246 conversion rate as input for the GSK3529246 transit compartment (Run 4); (iii) induction of active metabolite CL/F; and (iv) inclusion of weight as a covariate on V_1/F as also previously reported by Krishnatry et al.[20] Following this, Run 14 (Table 2) was selected as the combined structural PK model for covariate analysis.

Covariate analysis and final PK model

The GAM analysis indicated that age and weight may impact CL/F of both molibresib and GSK3529246 and that time-varying AST likely affected metabolite CL/F. A full model, including separate coefficients for age and weight effects on CL/F and mCL/F, was used for stepwise backward elimination, ultimately retaining weight as the covariate on V_1/F and mV_1/F and AST as a covariate on GSK3529246 CL/F. The final PK model includes body weight effects on V_1/F and mV_1/F and AST effects on mCL/F (Table S4). The final combined population PK model was Run 32 (graphical and mathematical representations in Figure 1). The semimechanistic liver-compartment autoinduction model consisted of (i) a lag-time,

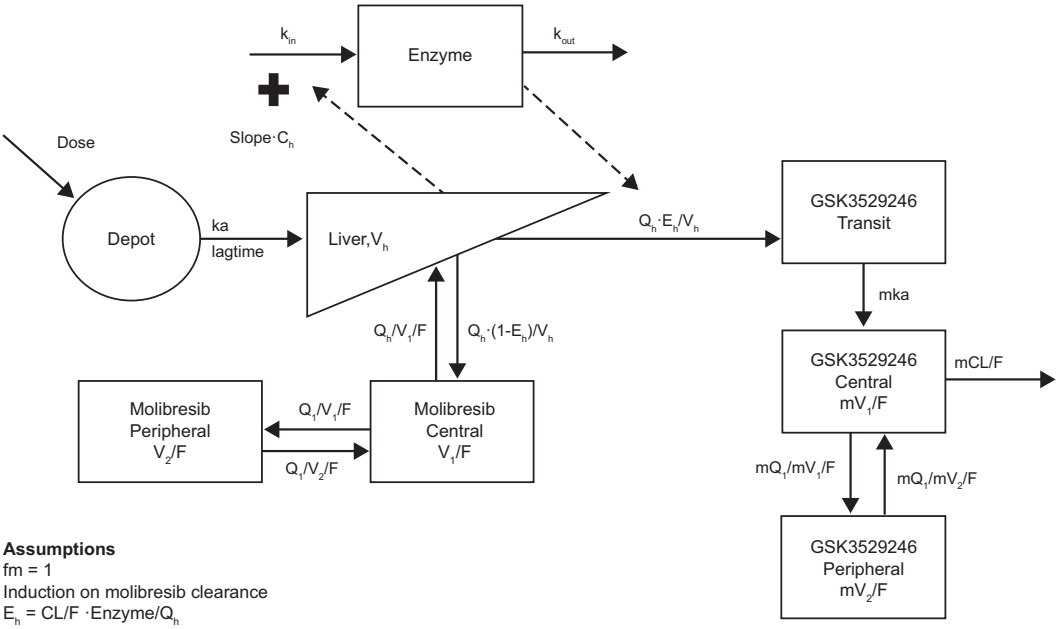

Assumptions
fm = 1
Induction on molibresib clearance
$E_h = CL/F \cdot Enzyme/Q_h$

$$\frac{dA_{depot}}{dt} = -ka \cdot A_{depot}$$

$$\frac{dA_{liver}}{dt} = ka \cdot A_{depot} - \frac{Q_h \cdot (1-E_h)}{V_h} \cdot A_{liver} + \frac{Q_h}{V_1/F} \cdot A_{central} - \frac{Q_h \cdot E_h}{V_h} \cdot A_{liver}$$

$$\frac{dA_{central}}{dt} = \frac{Q_h \cdot (1-E_h)}{V_h} \cdot A_{liver} - \frac{Q_h}{V_1/F} \cdot A_{central} + \frac{Q_1}{V_1/F} \cdot A_{central} + \frac{Q_1}{V_2/F} \cdot A_{peripheral}$$

$$\frac{dA_{peripheral}}{dt} = \frac{Q_1}{V_1/F} \cdot A_{central} - \frac{Q_1}{V_2/F} \cdot A_{peripheral}$$

$$\frac{dA_{enzyme}}{dt} = k_{in} \cdot (1 + induction) - k_{out} \cdot A_{enzyme}$$

$$\frac{dA_{Mtransit}}{dt} = \frac{Q_h \cdot E_h}{V_h} \cdot A_{liver} - mka \cdot A_{Mtransit}$$

$$\frac{dA_{Mcentral}}{dt} = mka \cdot A_{Mtransit} - \frac{mQ1}{mV_1/F} \cdot A_{Mcentral} + \frac{mQ1}{mV_2/F} \cdot A_{Mperipheral} - \frac{mCL/F}{mV_1/F} \cdot A_{Mcentral}$$

$$\frac{dA_{Mperipheral}}{dt} = \frac{mQ_1}{mV_1/F} \cdot A_{Mcentral} - \frac{mQ1}{mV_2/F} \cdot A_{Mperipheral}$$

$$induction = slope \cdot \left(\frac{A_{liver}}{V_h}\right)$$

$$E_h = \frac{CL/F \cdot A_{enzyme}}{Q_h}$$

FIGURE 1 Graphical and mathematical representations of the final population PK model components. Dashed lines indicate the effect of C_h on k_{in} and the effect of enzyme on clearance. $A_{central}$, molibresib amount in the central compartment; A_{depot}, molibresib amount in the absorption compartment; A_{enzyme}, enzyme amount; A_{liver}, molibresib amount in the liver compartment; $A_{Mtransit}$, GSK3529246 amount in the transit compartment; $A_{Mcentral}$, GSK3529246 amount in the central compartment; $A_{Mperipheral}$, GSK3529246 amount in the peripheral compartment; $A_{peripheral}$, molibresib amount in the peripheral compartment; C_h, molibresib concentration in the liver compartment; CL/F, molibresib clearance; E_h, hepatic extraction rate; Enzyme, enzyme amount; fm, fraction metabolized; ka, molibresib absorption rate constant; k_{in}, enzyme production rate; k_{out}, enzyme turnover rate; mCL/F, GSK3529246 clearance; mka, GSK3529246 absorption rate; mQ_1, GSK3529246 intercompartmental clearance; mV_1/F, GSK3529246 central volume; mV_2/F, GSK3529246 peripheral volume; PK, pharmacokinetic; Q_1, molibresib interpompartmental clearance; Q_h, liver plasma flow; slope, linear induction slope; V_1/F, molibresib central volume; Q_1, molibresib intercompartmental clearance; V_2/F, molibresib peripheral volume; V_h, liver volume (fixed to 1.5L)

first-order absorption, two-compartment model for molibresib with linear elimination; (ii) a two-compartment distribution model for GSK3529246, including a transit compartment to account for the delay in GSK3529246 formation; (iii) a physiologic liver compartment describing the elimination of molibresib; and (iv) an enzyme induction compartment (in which enzyme production is proportional to molibresib liver concentrations) that linearly alters the conversion of molibresib to GSK3529246. The model incorporated IIV on molibresib ka, CL/F, and V_1/F, and GSK3529246 mka, mCL/F, and mV_1/F as independent random effects. PK parameter estimates using the final model are presented in Table 3, and the model code is presented in Supplementary Text S2. The CL/F and mCL/F were estimated to be 9.02 L/h and 12.8 L/h, respectively. The V_1/F and mV_1/F were 53.1 L and 62.1 L, respectively.

Model qualification

The final model characterized the PK of molibresib and GSK3529246 with all parameters estimated with sufficient precision (i.e., a relative standard error <50%; Table 3). In addition, the model fulfilled successful numerical convergence and the condition number was low (47.8). Molibresib autoinduction was shown to be weak to moderate, with a 2.1-fold maximum increase in hepatic enzyme amount (based on the maximum estimate for any subject in the enzyme compartment of the final model [Run 32, 75 mg dose]). Given the limited PK data for GSK3529246 for the majority of patients in Part 1 of the study, this was as expected. The GOF plots for the final population PK model showed conditionally weighted residuals (CWRES) randomly scattered around the predicted range and across time and time after dose (Figure S2). Quantile–quantile and density plots of CWRES indicated normal distribution with a mean of ~0 and a variance of ~1 (Figure S3). Overall, the diagnostic GOF plots showed that the final population PK model demonstrated appropriate agreement between predicted and observed data for both molibresib and GSK3529246 and that there was no structural bias or substantial lack of fit. Prediction-corrected VPC also showed that the final model adequately described both molibresib and GSK3529246 over time following both single-dose and repeat-dose administration (Figure 2).

The impact of the covariates included in the final population PK model are presented in Figure 3a. Weight was shown to have a significant effect on the V_1/F of both molibresib and GSK3529246, with a lower weight leading to a lower distribution volume and vice versa. Weight was also shown to affect C_{max} and $t_{1/2}$, with a lower weight leading to an increased C_{max} and shorter $t_{1/2}$ and vice versa (Figure 3b, Table S5). In addition, AST levels were shown to affect GSK3529246 CL/F, with higher AST levels resulting in lower clearance.

Exposure predictions

Using the final PK model, individual exposure metrics (C_{max}, C_{min}, and area under the concentration versus time curve between 0 and 24 h postdose [$AUC_{0-24\ h}$]) were predicted for single-dose (Week 1, Day 1) and repeat-dose administrations (Week 3, Day 4) for molibresib, GSK3529246, and TAM (molibresib+GSK3529246). Exposure metrics for the selected doses are presented in Table 4.

DISCUSSION

We developed a semimechanistic liver-compartment population PK model that adequately describes the PK of both molibresib and GSK3529246, including the autoinduction indicated by preliminary PK analyses.[18] Molibresib is mostly eliminated by CYP3A4-mediated metabolism, which produces two major active metabolites that are equipotent to the parent molecule; these were measured together following full conversion of one to the other and reported as GSK3529246.[19] An *in vitro* study conducted to evaluate the effects of molibresib on CYP3A4 expression in primary human hepatocytes showed a concentration-dependent increase in CYP3A4 mRNA was induced by molibresib (up to 300 μM) in all three donors tested with molibresib and in one donor with GSK3529246 (unpublished data on file). PK data obtained from Part 1 of the FTIH study showed a decreased exposure of molibresib with repeat dosing ≥60 mg q.d., suggesting autoinduction of molibresib metabolism.[18] An empirical population PK model for molibresib was developed using preliminary data from Part 1 of the FTIH study,[20] describing the autoinduction of molibresib clearance based on a similar model describing the autoinduction of artemisinin.[20,28] In the work presented here, the analysis was expanded by including the full data set (n = 193 patients; both Part 1 and Part 2) from the FTIH study that not only includes the exposure of molibresib as per the empirical model but also includes the exposure of the active metabolite composite, GSK3529246. The final semimechanistic PK model includes an enzyme induction compartment that linearly alters conversion of molibresib to GSK3529246 and included a two-compartment model for molibresib and GSK3529246 with first-order elimination for GSK3529246. An additional GSK3529246 transit compartment was linked to the central molibresib compartment to account for delayed formation of GSK3529246. The model incorporated IIV on ka, CL/F, V_1/F, mka, mCL/F, and mV_1/F as independent variables. Conversion of molibresib into GSK3529246 (CL/F) was proportional to the amount of enzyme in the enzyme pool compartment with an up to 2.1-fold increase. Other linear and nonlinear models were tested, but these did not improve the model fit or resulted in worsening of the

TABLE 3 Final model PK parameter estimates (Run 32)

Description	Parameter (unit)	Estimate	RSE (%)	95% CI	IIV (%)
Molibresib absorption rate	ka (/h)	4.08	…	3.27–5.1	…
Molibresib clearance	CL/F (L/h)	9.02	…	8.34–9.76	…
Molibresib central volume of distribution	V_1/F (L)	53.1	…	49.4–57	…
Liver plasma flow	Q_h (L/h)	55.0	…	Fixed	…
Liver volume	V_h/F (L)	1.50	…	Fixed	…
Molibresib intercompartmental clearance	Q_1 (L/h)	0.999	…	0.774–1.29	…
Molibresib peripheral volume of distribution	V_2/F (L)	17.4	…	14.3–21.2	…
Lagtime	ALAG (h)	0.132	…	0.118–0.149	…
Induction slope	Slope	0.922	…	0.687–1.24	…
Enzyme production rate	k_{in} (/h)	0.00550	…	Fixed	…
GSK3529246 transit rate	mka (/h)	11.5	…	7.76–17.1	…
GSK3529246 clearance	mCL/F (L/h)	12.8	…	11.5–14.4	…
GSK3529246 central volume of distribution	mV_1/F (L)	62.1	…	55.2–69.7	…
GSK3529246 intercompartmental clearance	mQ_1 (L/h)	5.63	…	4.04–7.84	…
GSK3529246 peripheral volume of distribution	mV_2/F (L)	140	…	104–188	…
Weight effect on V_1/F and mV_1/F	WT on V_1/F and mV_1/F	0.717	5.70	0.637–0.796	…
AST effect on mCL/F	AST on mCL/F	−0.194	34.3	−0.324 to −0.0635	…
IIV on absorption rate	ω^2_{ka}	1.65	15.2	1.16–2.14	128
IIV on molibresib clearance	$\omega^2_{CL/F}$	0.205	14.4	0.147–0.263	45.3
IIV on molibresib central volume of distribution	$\omega^2_{V1/F}$	0.0687	25.1	0.0348–0.103	26.2
IIV on GSK3529246 transit rate	ω^2_{mka}	0.488	43.3	0.0741–0.903	69.9
IIV on GSK3529246 clearance	$\omega^2_{mCL/F}$	0.227	16.5	0.154–0.3	47.6
Covariance IIV mCL and mV	$\omega^2_{\mathrm{mCL/F,mV1/F}}$	174	19.5	0.107–0.24	…
IIV on GSK3529246 central volume of distribution	$\omega^2_{\mathrm{mV1/F}}$	0.206	23.3	0.112–0.3	45.4
Proportional error molibresib	$\sigma_{prop-molibresib}$	0.207	7.40	0.177–0.237	…
Correlation error molibresib and GSK3529246	correlation $\sigma_{molibresib-GSK3529246}$	0.0918	15.7	0.0635–0.12	…
Proportional error GSK3529246	$\sigma_{prop-GSK\ 3529246}$	0.132	10.9	0.104–0.16	…

Note: For log-transformed parameters, the RSE is only available for the log-scale and is not reported on the normal scale.

Abbreviations: ω^2_X, variance of the IIV of parameter X; $\omega^2_{X,Y}$, covariance of the IIV of parameters X and Y; AST, aspartate aminotransferase; CI, confidence interval; IIV, interindividual variability (derived from the variance according to $\sqrt{\omega^2_X}\cdot 100$); PK, pharmacokinetic; RSE, relative standard error; WT, weight.

fit. The linear induction model was selected as the nonlinear maximal effect model was not superior to the linear model and resulted in parameter identifiability issues. Furthermore, induction was tested on parent clearance, metabolite clearance, and a combination of the two, with the model only affecting parent clearance. Consequently, bioavailability, through a decrease in the fraction escaping hepatic elimination (Fh), was also affected by parent clearance induction ($Fh = 1-E_h = [CL/F]/Q_h$). The increase in the amount of enzyme in the pool compartment was driven by an increased synthesis rate, which in turn was driven by the amount of molibresib present in the liver. Consequently, elevated enzyme amounts led to increased hepatic extraction and accelerated elimination of molibresib and formation of the active metabolites. The final PK model also included the assumption that presystemic exposure would significantly contribute to the autoinduction effect, with each successive dose of molibresib affecting hepatic enzymes to a similar degree, contrary to successively diminished systemic exposures. According to the well-stirred liver model,[29] the clearance of molibresib was low (CL/F of 9.02 L/h) relative to the hepatic plasma flow (55 L/h), which indicates a low

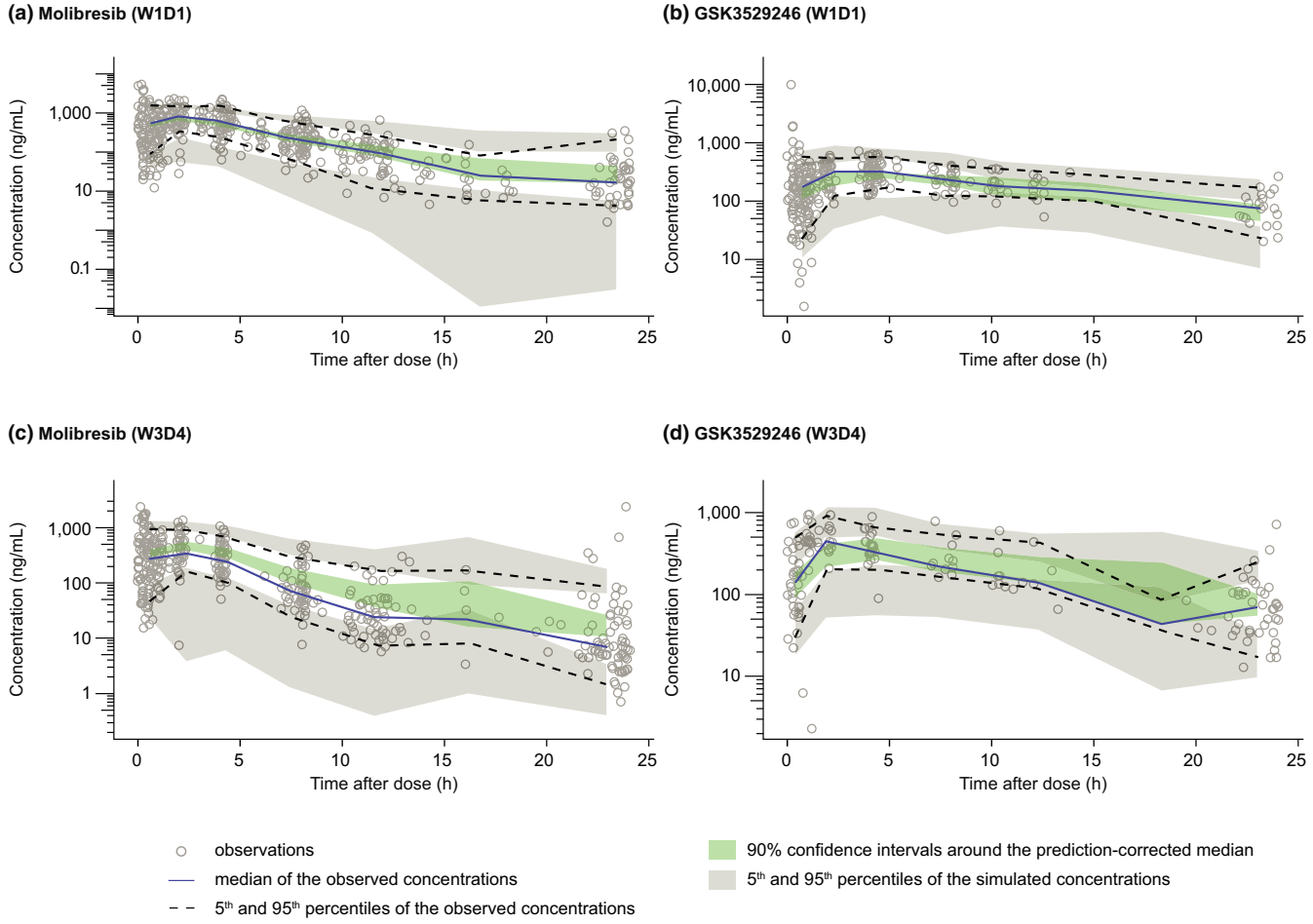

FIGURE 2 VPC using the final PK model for single and repeat administrations of molibresib (a,c) and GSK3529246 (b,d). All observations and predictions were adjusted using prediction correction.[27] Bootstrap analyses were not performed due to the long run times of the PK model. PK, pharmacokinetic; VPC, Visual predictive check; W1D1; Week 1, Day 1; W3D4, Week 3, Day 4

hepatic extraction ratio. It was interesting to note that the peripheral distribution volume for GSK3529246 (mV2/F = 140 L) was much larger compared with molibresib (V2/F = 17 L), although both have similar plasma protein binding and physico-chemical properties. It is possible that conformational changes, steric effects, or active transport could explain the apparent greater GSK3529246 tissue binding. Despite their similar structure, the disposition and elimination of molibresib and GSK3529246 appear to be different, something that was further substantiated by the observation that autoinduction on the metabolite elimination pathway was not supported by the data.

In the final population PK model, body weight (ranging from 34 to 120 kg) was shown to have a significant effect on the V_1/F of both molibresib and GSK3529246, with a lower weight leading to a lower distribution volume and vice versa (Figure 3). As such, a patient's weight is expected to have a large impact on their exposure to molibresib and GSK3529246 and needs to be evaluated further with exposure–response analyses to determine if dose adjustment based on weight is indicated. In contrast, although time-varying AST was shown to have an effect on mCL/F in the final population PK model, with higher AST levels leading to lower clearance and vice versa, the change in OFV (12.9 points) was only marginally greater than the threshold for significance (10.8 points, equivalent to $p < 0.001$ with one degree of freedom). The impact of AST on mCL/F was relatively small, indicating that the impact on exposure to GSK3529246 may not be clinically meaningful (Figure 3).

A bottom-up approach (i.e., a PBPK model) was also developed in addition to the population PK model and has been described in a recent publication by Riddell et al.[19] This type of PK modeling approach, in which each compartment has a physiological representation (such as an organ or tissue) and is interconnected via the blood circulation is easier to conceptualize than a population PK approach. This approach has been increasingly used to predict drug–drug interactions. For example, the PBPK model simulations of molibresib enabled drug interactions with itraconazole and rifampicin to be evaluated, thereby minimizing plasma exposures in healthy

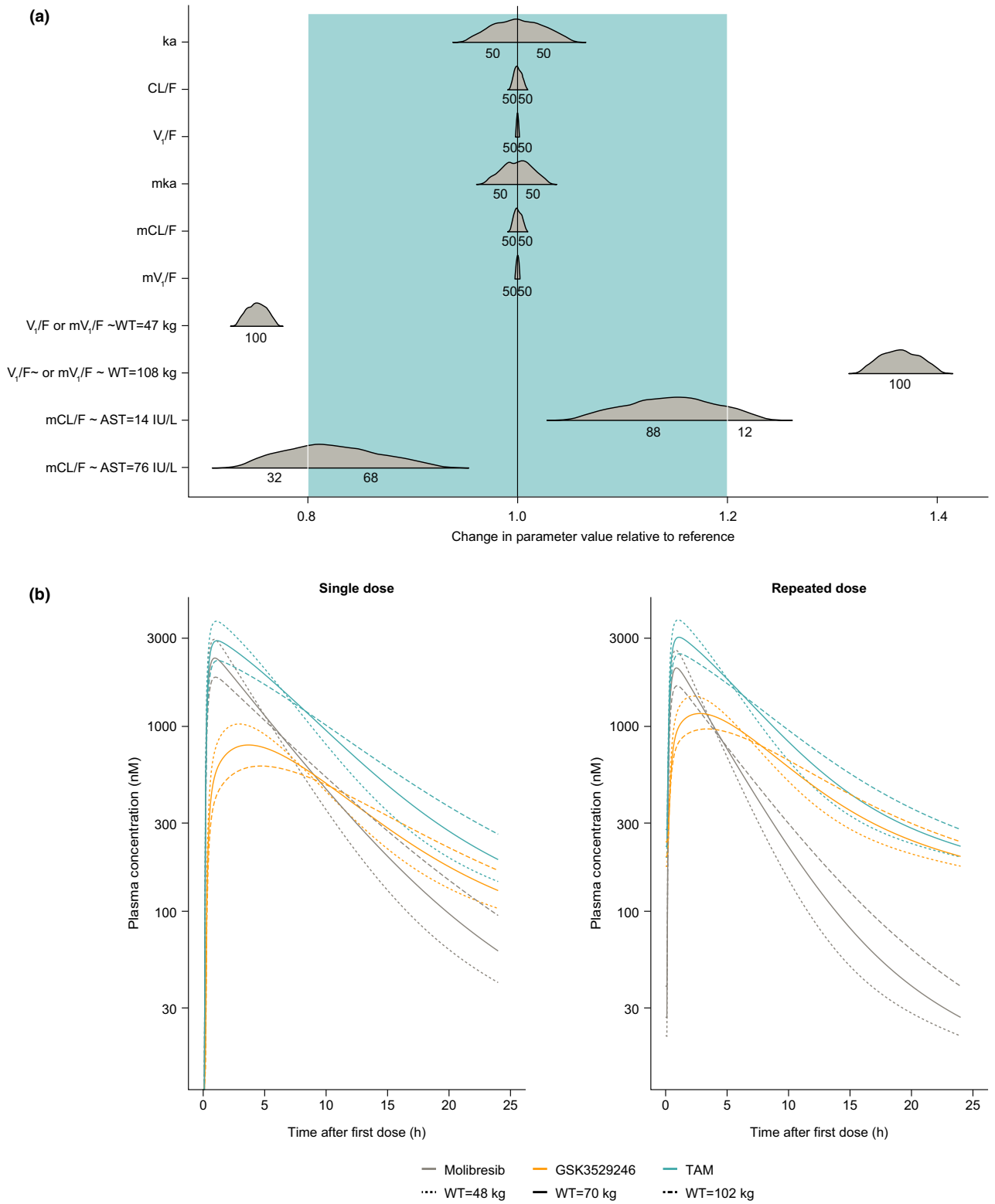

FIGURE 3 For the final PK population model, (a) the effect of weight and AST on posterior PK parameter distributions ($n = 1000$ simulations) and (b) predicted molibresib, GSK3529246, and TAM concentration–time profiles following single-dose and repeat-dose (once-daily) administration of 75 mg molibresib. (a) Lower and higher covariate cut-off values for WT and AST are based on the observed 5th and 95th percentiles of the patients included in the FTIH study. The probabilities of covariates to clinically impact pharmacokinetic parameters (defined as a 20% change from the typical value [blue area]) are displayed for each distribution. (b) WT categories represent the 5th and 95th percentiles of the WT distribution observed in the FTIH study. AST, aspartate aminotransferase; CL/F, molibresib clearance; FTIH, first-time-in-human; ka, molibresib absorption rate constant; mCL/F, GSK3529246 clearance; mka, GSK3529246 absorption rate; mV_1/F, GSK3529246 central volume; PK, pharmacokinetic; TAM, total active moiety; V_1/F, molibresib central volume; WT, weight

TABLE 4 Summary statistics for the predicted individual exposure metrics (A) C_{max}, (B) C_{min}, and (C) $AUC_{0-24\ h}$ for W1D1 and W3D4

			C_{max} molibresib (ng/ml)		C_{max} GSK3529246 (ng/ml)		C_{max} TAM (nM)	
Part and dose	**Day**	***n***	**Mean**	**Range**	**Mean**	**Range**	**Mean**	**Range**
Part 1—40 mg b.i.d.	W1D1	5	517.0	402–769	222.0	169–263	1700	1550–2240
	W3D4	3	457.0	334–668	365.0	328–395	1900	1650–2350
Part 1—60 mg q.d.	W1D1	9	680.0	434–824	296.0	205–400	2220	1830–2480
	W3D4	7	628.0	458–829	379.0	310–450	2290	1910–2680
Part 1—80 mg q.d.	W1D1	32	933.0	433–1480	355.0	83.4–721	2890	1700–4580
	W3D4	19	775.0	449–1600	448.0	199–1020	2790	1680–4990
Part 1—100 mg q.d.	W1D1	9	920.0	605–1280	383.0	140–513	2970	2060–3920
	W3D4	6	810.0	515–1060	567.0	404–676	3220	2450–3930
Besylate substudy—80 mg q.d.	W1D1	10	1160.0	577–2170	316.0	201–428	3280	2210–5450
	W3D4	10	1060.0	552–1990	469.0	392–578	3480	2560–5500
Part 2—75 mg q.d.	W1D1	99	935.0	445–1770	325.0	118–738	2840	1420–5060
	W3D4	55	785.0	364–1400	431.0	149–1320	2780	1310–5970
			C_{min} molibresib (ng/ml)		C_{min} GSK3529246 (ng/ml)		C_{min} TAM (nM)	
			Mean	**Range**	**Mean**	**Range**	**Mean**	**Range**
Part 1—40 mg b.i.d.	W1D1	5	55.9	30.5–97.2	94.5	48–124	373.0	194–545
	W3D4	3	19.2	14.2–22.2	128.0	83.8–159	368.0	246–455
Part 1—60 mg q.d.	W1D1	9	5.7	1.01–14.4	21.3	16.5–25.7	67.2	44.2–98.1
	W3D4	7	10.2	1.31–23.7	57.7	38.1–73.4	170.0	99.4–242
Part 1—80 mg q.d.	W1D1	32	47.7	3.78–323	65.8	13.8–172	279.0	43.7–932
	W3D4	19	12.3	1.97–84.8	66.1	19.7–184	196.0	56.2–580
Part 1—100 mg q.d.	W1D1	9	33.6	2–220	46.8	25.6–94.7	198.0	69.4–759
	W3D4	6	51.4	3.54–261	120.0	54–246	426.0	145–1240
Besylate substudy—80 mg q.d.	W1D1	10	22.2	3.12–99.2	34.7	27.4–52.3	140.0	89.7–366
	W3D4	10	22.7	5.47–82.6	89.6	48.2–124	280.0	135–509
Part 2—75 mg q.d.	W1D1	99	40.9	2.87–331	57.5	8.18–222	242.0	27.5–1330
	W3D4	55	22.7	2.13–279	82.7	13.5–689	263.0	39.2–2060
			AUC_{0-24} molibresib (ng/ml)		AUC_{0-24} GSK3529246 (ng/ml)		AUC_{0-24} TAM (nM·h)	
			Mean	**Range**	**Mean**	**Range**	**Mean**	**Range**
Part 1—40 mg b.i.d.	W1D1	5	2790	2430–3280	1860.0	1440–2200	11300	9640–12200
	W3D4	3	3240	2800–4050	5810.0	5090–6510	22300	21500–23100
Part 1—60 mg q.d.	W1D1	9	3600	1890–5320	2640.0	2250–2940	15200	11500–18300
	W3D4	7	3170	1580–4780	4240.0	3860–4500	18200	13500–22100
Part 1—80 mg q.d.	W1D1	32	5290	2680–12100	3230.0	808–6490	20600	12100–40100
	W3D4	19	3500	2220–6140	4730.0	2250–10400	20200	12200–34400
Part 1—100 mg q.d.	W1D1	9	5980	3100–8440	3910.0	1680–4560	24000	18500–29000
	W3D4	6	5350	2470–12800	6970.0	5190–7920	30200	19000–50300
Besylate substudy—80 mg q.d.	W1D1	10	6610	3000–12000	3110.0	1840–3890	23500	16900–36500
	W3D4	10	5470	2570–10600	5890.0	5080–7030	27800	23600–40600
Part 2—75 mg q.d.	W1D1	99	5260	2460–10700	2720.0	889–6750	19300	9300–34100
	W3D4	55	4330	1790–13100	5010.0	1340–23000	22900	9810–86700

Note: Not all subjects received active treatment between Day 18 an Day 21; therefore, fewer exposure estimates are available for W3D4.

Abbreviations: $AUC_{0-24\ h}$, area under the concentration versus time curve between 0 and 24 h postdose; b.i.d., twice daily; C_{max}, maximum plasma concentration; C_{min}, minimum concentration; GSK3529246, combined major metabolites of molibresib; NA, not calculated; q.d., once daily; TAM, total active moiety (molibresib +GSK3529246); W1D1, first day of treatment (Week 1, Day 1); W3D4, predictions for the first day with active treatment between Day 18 and Day 21 (Week 3, Day 4).

subjects. However, the PBPK modeling approach is limited by its complexity, requiring the inclusion of many parameters such as organ volumes and blood flows, partition coefficients and compound/species-specific elimination. Many of these parameters cannot be calculated and are often based on *in vitro* estimates, preclinical data, and values sourced from available literature.

In contrast, the population PK model described here uses a top-down approach and is based on the characterization of observed clinical data. Although population PK models are rather empirical compared with PBPK models, the developed molibresib population PK model is semiphysiological and includes a liver compartment, comparable to a PBPK model with actual liver volume and blood flow. One of the advantages of the population PK model is its capability to identify intrinsic and extrinsic sources of PK and exposure variability, such as weight, sex, and organ function, along with quantifying the unexplained interpatient variability in disposition and elimination parameters. Both PBPK and population PK models are complementary regarding their descriptive and predictive properties, and depending on the specific type of question that needs to be addressed, one can use one or the other. Although a more complex PBPK model may be employed to evaluate dose scaling or drug–drug interactions, a population PK model is particularly useful in evaluating intrinsic/extrinsic factors affecting the PK as well as describing individual PK profiles to inform safety and efficacy analyses.

Strengths of the population PK modeling analysis described here include the inclusion of both molibresib and metabolite concentration into the model as well as a hepatic autoinduction mechanism for molibresib. Plasma concentration-driven autoinduction would result in a decrease in enzyme induction due to decreased plasma exposures and would therefore not be appropriate. Another strength is the ability of the semimechanistic model to identify covariates of clinical interest and describe the time-course over a wide range of doses and concentrations. The semimechanistic liver model may also provide information on the hepatic extraction ratio in addition to changes in enzyme activity. Overall, by providing a means of describing individual molibresib and GSK3529246 PK over time, exposure–response analyses, including time-course analysis, can be performed to further characterize the effect of molibresib in various patient populations. One limitation of the study is that metabolite data were only available for a limited number of patients in Part 1 (80 mg only, $n = 32$). Another limitation is the apparent underprediction of the model revealed in some of the GOF plots for Part 2 of the FTIH study (Figure S2). This may be attributed to the use of patient diaries in the expansion cohort, potentially resulting in inaccurate recordings, or interoccasion variability in absorption leading to higher C_{max} levels.

In conclusion, a semimechanistic liver-compartment population PK model including autoinduction of molibresib clearance adequately describes the PK of both molibresib and its active metabolite composite, GSK3529246. This model can be used to simulate individual patient exposures based on covariate information for use in alternative dosing strategy and combination studies and has already been employed in an exposure–response analysis (evaluating the impact of the drug on platelet count, QT interval, and gastrointestinal adverse events) of molibresib using data from the FTIH study. Results of this analysis will be published separately.

ACKNOWLEDGMENTS

Editorial support (in the form of writing assistance, including development of the initial draft based on author direction, assembling tables and figures, collating authors' comments, grammatical editing, and referencing) was provided by Anna Polyakova, PhD, and Stuart Wakelin, PhD, of Fishawack Indicia Ltd, UK, and was funded by GlaxoSmithKline.

CONFLICT OF INTEREST

A.S.K. is an employee of GlaxoSmithKline (GSK) and hold stocks/shares in GSK. A.V. is an employee of qPharmetra LLC. A.D. has a family member employed by PRA Health Sciences, is an employee of GSK, and holds stocks/shares in GSK. M.P. is an employee of qPharmetra LLC. G.F.-B. is an employee of GSK and holds stocks/shares in GSK.

AUTHOR CONTRIBUTIONS

A.S.K., A.V., A.D., M.P., and G.F.-B. wrote the manuscript. A.S.K., A.V., A.D., M.P., and G.F.-B. designed the research. A.S.K., A.V., A.D., M.P., and G.F.-B. performed the research. A.S.K., A.V., A.D., M.P., and G.F.-B. analyzed the data.

DATA AVAILABILITY STATEMENT

Anonymized individual participant data and study documents can be requested for further research from www.clinicalstudydatarequest.com.

REFERENCES

1. Nicodeme E, Jeffrey KL, Schaefer U, et al. Suppression of inflammation by a synthetic histone mimic. *Nature*. 2010;468:1119–1123.
2. Zhao Y, Yang CY, Wang S. The making of I-BET762, a BET bromodomain inhibitor now in clinical development. *J Med Chem*. 2013;56:7498–7500.
3. Muller S, Filippakopoulos P, Knapp S. Bromodomains as therapeutic targets. *Expert Rev Mol Med*. 2011;13:e29.
4. Perez-Salvia M, Esteller M. Bromodomain inhibitors and cancer therapy: From structures to applications. *Epigenetics*. 2017;12:323–339.
5. Mujtaba S, Zeng L, Zhou MM. Structure and acetyl-lysine recognition of the bromodomain. *Oncogene*. 2007;26:5521–5527.

6. Filippakopoulos P, Picaud S, Mangos M, et al. Histone recognition and large-scale structural analysis of the human bromodomain family. *Cell*. 2012;149:214–231.
7. Dey A, Nishiyama A, Karpova T, McNally J, Ozato K. Brd4 marks select genes on mitotic chromatin and directs postmitotic transcription. *Mol Biol Cell*. 2009;20:4899–4909.
8. Yang Z, He N, Zhou Q. Brd4 recruits P-TEFb to chromosomes at late mitosis to promote G1 gene expression and cell cycle progression. *Mol Cell Biol*. 2008;28:967–976.
9. Manzotti G, Ciarrocchi A, Sancisi V. Inhibition of BET proteins and histone deacetylase (HDACs): Crossing roads in cancer therapy. *Cancers (Basel)*. 2019;11:304.
10. Wyce A, Soden P, Felitsky DJ, et al. Mechanism-based combination strategies for BET inhibitors in NUT midline carcinoma. Paper presented at: American Association for Cancer Research Annual Meeting; December 6–10, 2016; New Orleans, LA.
11. Wyce A, Matteo JJ, Foley SW, et al. MEK inhibitors overcome resistance to BET inhibition across a number of solid and hematologic cancers. *Oncogenesis*. 2018;7:35.
12. Wyce A, Degenhardt Y, Bai Y, et al. Inhibition of BET bromodomain proteins as a therapeutic approach in prostate cancer. *Oncotarget*. 2013;4:2419–2429.
13. Asangani IA, Dommeti VL, Wang X, et al. Therapeutic targeting of BET bromodomain proteins in castration-resistant prostate cancer. *Nature*. 2014;510:278–282.
14. Zhang D, Leal AS, Carapellucci S, Zydeck K, Sporn MB, Liby KT. Chemoprevention of Preclinical Breast and Lung Cancer with the Bromodomain Inhibitor I-BET 762. *Cancer Prev Res (Phila)*. 2018;11:143–156.
15. Ocana A, Nieto-Jimenez C, Pandiella A. BET inhibitors as novel therapeutic agents in breast cancer. *Oncotarget*. 2017;8:71285–71291.
16. Stuhlmiller TJ, Miller SM, Zawistowski JS, et al. Inhibition of lapatinib-induced kinome reprogramming in ERBB2-positive breast cancer by targeting BET family bromodomains. *Cell Rep*. 2015;11:390–404.
17. Hemming ML, Lawlor MA, Andersen JL, et al. Enhancer domains in gastrointestinal stromal tumor regulate KIT expression and are targetable by BET bromodomain inhibition. *Cancer Res*. 2019;79:994–1009.
18. Piha-Paul SA, Hann CL, French CA, et al. Phase 1 Study of Molibresib (GSK525762), a bromodomain and extra-terminal domain protein inhibitor, in NUT carcinoma and other solid tumors. *JNCI Cancer Spectr*. 2020;4(2):1–9.
19. Riddell K, Patel A, Collins G, et al. An adaptive physiologically based pharmacokinetic-driven design to investigate the effect of itraconazole and rifampicin on the pharmacokinetics of molibresib (GSK525762) in healthy female volunteers. *J Clin Pharmacol*. 2021;61(1):125–137.
20. Krishnatry AS, Harward SD, Horner T, et al. Population pharmacokinetics and pharmacodynamics of GSK525762 in patients with solid tumors. Paper presented at: 26th annual meeting of the Population Approach Group Europe; June 6–9, 2017; Budapest, Hungary.
21. Lindbom L, Pihlgren P, Jonsson EN. PsN-Toolkit–a collection of computer intensive statistical methods for non-linear mixed effect modeling using NONMEM. *Comput Meth Programs Biomed*. 2005;79:241–257.
22. R Development Core Team. R: A language and environment for statistical computing. http://www.R-project.org. Accessed July 3, 2020.
23. Food and Drug Administration (FDA). *In vitro* metabolism and transporter-mediated drug-drug interaction studies: guidance for industry. https://www.fda.gov/media/108130/download. Accessed July 4, 2020.
24. Salazar Vazquez BY, Salazar Vazquez MA, Chavez-Negrete A, et al. Influence of serological factors and BMI on the blood pressure/hematocrit association in healthy young men and women. *Vascular Health Risk Manag*. 2014;10:271–277.
25. Wynne HA, Cope LH, Mutch E, Rawlins MD, Woodhouse KW, James OF. The effect of age upon liver volume and apparent liver blood flow in healthy man. *Hepatology*. 1989;9:297–301.
26. National Institute of Standards and Technology and Semiconductor Manufacturing Technology (NIST/SEMATECH). e-Handbook of Statistical Methods. Section 1.3.6.7.4. Critical values of the chi-square distribution. https://www.itl.nist.gov/div898/handbook/eda/section3/eda3674.htm. Accessed October 9, 2020.
27. Bergstrand M, Hooker AC, Wallin JE, Karlsson MO. Prediction-corrected visual predictive checks for diagnosing nonlinear mixed-effects models. *AAPS J*. 2011;13:143–151.
28. Gordi T, Xie R, Huong NV, Huong DX, Karlsson MO, Ashton M. A semiphysiological pharmacokinetic model for artemisinin in healthy subjects incorporating autoinduction of metabolism and saturable first-pass hepatic extraction. *Br J Clin Pharmacol*. 2005;59:189–198.
29. Smith DA, Beaumont K, Maurer TS, Di L. Clearance in drug design. *J Med Chem*. 2019;62:2245–2255.

SUPPORTING INFORMATION

Additional supporting information may be found online in the Supporting Information section.

How to cite this article: Krishnatry AS, Voelkner A, Dhar A, Prohn M, Ferron-Brady G. Population pharmacokinetic modeling of molibresib and its active metabolites in patients with solid tumors: A semimechanistic autoinduction model. *CPT Pharmacometrics Syst. Pharmacol.* 2021;10:709–722. https://doi.org/10.1002/psp4.12639